Journal of Applied Polymer Science

Attapulgite-Supported Aluminum Oxide Hydroxide Catalyst for Synthesis of Poly(ethylene terephthalate)

Qinghui Lin, Yiqing Gu, Dajun Chen
State Key Laboratory for Modification of Chemical Fibers and Polymer Materials, College of Materials Science and Engineering, Donghua University, Shanghai 201620, China
Correspondence to: D. Chen (E-mail: cdj@dhu.edu.cn)

ABSTRACT: A novel nanocomposite catalyst was prepared from immobilization of aluminum oxide hydroxide onto the attapulgite. Characterizations with scanning electron microscopy (SEM) and wide angle X-ray diffraction (XRD) of the as-prepared catalyst revealed that AlO(OH) nanoparticles were distributed on the attapulgite. Thermogravimetric analysis-infrared spectrometry (TGA-IR) of the mixture prepared by mixing of bishydroxy ethylene terephthalate (BHET) and the catalyst indicated that attapulgite-supported aluminum oxide hydroxide catalyst can catalyze BHET polycondensation under the applied conditions. A kinetic model for determining the activation energy has been applied to evaluate the catalyst activity. The catalyst activity was examined through comparative experiments, and the results showed that the new catalyst exhibited higher activity for BHET polycondensation under identical reaction conditions, and the viscosity-average molecular weight of poly(ethylene terephthalate) (PET) product obtained was increased about 2000 g/mol. © 2013 Wiley Periodicals, Inc. J. Appl. Polym. Sci. 129: 2571–2579, 2013

KEYWORDS: polycondensation; catalysts; kinetics; polyesters

Received 16 November 2012; accepted 28 December 2012; published online 30 January 2013
DOI: 10.1002/app.38973

INTRODUCTION

Poly(ethylene terephthalate) (PET) is the most common thermoplastic polyester. PET has numerous applications, with more than 85% being processed into fibers, while a significant and growing application of PET is the manufacture of gastight bottles for carbonated beverages.[1] PET is nowadays obtained commercially mainly by direct esterification of terephthalic acid (hereinafter abbreviated as TPA) with ethylene glycol (EG) followed by polycondensation of the esterification products, bishydroxy ethylene terephthalate (BHET), and its oligomers.

Polycondensation rate is influenced by the catalyst, and it is controlled by the removal of the byproduct EG. The esterification reaction does not require a catalyst, but the reaction can be accelerated in the presence of suitable catalysts for esterification. Catalysis plays a critical role in enhancing the rate of the polycondensation reaction,[2] so the research on new catalysts has never been interrupted.

Antimony oxide (and derivatives thereof) is utilized to catalyze the polycondensation step in most of PET plants because it demonstrates a good balance of catalytic activity, product quality, and cost. However, the use of antimony compounds is an important health risk especially when PET is used for food packaging. Although at present studies on the toxicity for humans are not enough, some indications that antimony trioxide could interfere with embryonic and fetal development exist.[3] Therefore, the search for a new antimony-free PET polycondensation catalyst with low environmental impact has been a very important task.

The titanium-based catalysts have been widely investigated over the last 40 years or more. The first generation of titanium-based catalysts, such as tetrabutyl titanate or isopropyl titanate, is very active relative to antimony. Although they were found to enhance reaction rates, they were prone to hydrolysis, which have reduced activity and yielded polymers of yellow color. After the 1970s, the research was focused on the modification of titanium-based catalysts, and some results have been achieved.[4,5] However, titanium-based catalysts still need to be optimized to have a good balance of reaction rate, end-product quality, and cost.

In recent years, the study on the aluminum-based catalysts for PET polycondensation has aroused more and more attention. The zeolites have ever been used to improve the mechanical properties of PET as additives in early times and were later found that they have some catalytic activity in PET

Additional Supporting Information may be found in the online version of this article.

polycondensation. It is important that the water content in the zeolite originates from the zeolite production in which the zeolite is only partially dewatered and not dried.[6] The research results show that the aluminum element plays the major role in the polycondensation reaction. It is feasible to improve the thermal stability and color of yield polymers by adding the cobalt salts and phosphate compounds like other catalyst system.[6,7]

It is known that the aluminum-based catalysts are generally inferior to antimony-based catalysts in catalyzing PET polycondensation under the same conditions (the same polycondensation reaction time, the same amount of catalysts, etc). To solve the problems that the catalytic activity is not practically sufficient when compared with the antimony compounds and titanium compounds, the patent[8] discloses that an aluminum compound, though being originally inferior in the catalytic activity, came to have a sufficient activity by allowing a phosphorus compound to be coexistent therewith. However, the phosphorus compounds described above are mostly toxic, which will bring new problems to PET plants. At the present time, the aluminum-based catalysts still have some shortcomings (yielded polymers of poor color, low molecular weight, etc), and they have not been utilized to catalyze the polycondensation step in most of PET plants.

Attapulgite (hereinafter abbreviated as AT), a species of hydrated magnesium aluminum silicate mineral $[(OH_2)_4(Mg, Al, Fe)_5(OH)_2Si_8O_{20}{\cdot}4H_2O]$ with unique chain structure, is characterized by high specific surface area, sorptivity, and decolorizing power.[9] AT has a wide variety of industrial applications. In the polyester industry, the addition of AT could improve the tensile strength and storage modulus, accelerate the crystallization rate, and enhance the thermal stability of PET.[10,11] It has been confirmed that TPA and EG can react with the hydroxyl group on the AT surface, and some PET molecules can be grafted onto AT through chemical bonding rather than physical absorption.[10] Therefore, it is possible that AT can influence the reaction rate of PET polycondensation.

It has been found that Aluminum oxide hydroxide [AlO(OH)] can be used as a dehydrating reagent for methanol, and the activity of AlO(OH) catalyst do not clearly change with the different reactive temperature.[12] Nevertheless, to the best of our knowledge, the catalyst which will have a sufficient activity for PET polycondensation by allowing AT to be coexistent therewith has not been reported.

It is valuable to search for a method for fast screening activity of different catalysts for polycondensation of BHET to PET. A method which is based on differential scanning calorimetry (DSC) has been developed by Wolf et al.[13] in 1978 to screen catalysts for polycondensation of BHET to PET. In 1986, Bhatty and coworkers[14] introduced thermogravimetric analysis (TGA) as a catalyst screening aid. An optimized method which is based on simultaneous gravimetric and calorimetric thermal analysis (TG/DSC–STA) has been applied to study the activity of a new polycondensation heterogeneous catalyst based on hydrotalcite by El-Toufaili et al. in 2005.[15] However, all the above methods were not associated with the experimental data of different heating conditions, and as a result they were not enough rigorous. To develop a suitable catalyst, the kinetics of the reactions has to be analyzed.[16] Actually, it is helpful that the kinetic data are used for the interpretation of reaction mechanisms and catalytic phenomena.[17]

In the present work, we have developed a new environmentally friendly catalyst for PET polycondensation, using AT as the support material for immobilization of aluminum oxide hydroxide. We have also proposed a convenient and rigorous method for fast evaluating the catalyst activity. The catalyst activity for polycondensation of BHET to PET has been examined through comparative experiments.

EXPERIMENTAL

Materials

BHET (>85%) was purchased from TOKYO Chemical Industry Co., Ltd and $NaAlO_2$ ($Al_2O_3\% \geq 41\%$) from Sinopharm Chemical Reagent Co., Ltd. The AT clay powder was kindly supplied by Jiangsu Jiu Chuan Nanomaterial Technology Co., Ltd. All the applied chemicals were used without further purification.

Catalyst Preparation

The preparation procedure of AT-supported aluminum oxide hydroxide (hereinafter abbreviated as aluminum oxide hydroxide/AT) catalyst can be described as follows: a given weight of AT was dispersed in deionized water (1 g AT/100 mL H_2O) and mixed with 100 ml sodium aluminate solution (with 4.1 g $NaAlO_2$) by ultrasonication for 30 min at room temperature, followed by slowly acidified to about pH 7 with HCl (0.5 mol/L) while stirring. After finishing the reaction, the resultant mixture was centrifuged at 10,000 rpm until the nanocomposite product was precipitated. Then, the product was washed with deionized water successively and separated again by centrifugation. This dispersion–precipitation procedure was repeated until chloride ion was removed. The resulting solid product was dried in a vacuum for about 20 h at 65°C and then milled to 200 mesh powders.

To compare the catalytic activity between the as-prepared catalyst and aluminum hydroxide catalyst, the aluminum hydroxide was obtained in the same manner as above method except that the AT was not added.

Catalyst Characterization

The surface morphologies of aluminum oxide hydroxide/AT were observed by field emission scanning electron microscopy (FESEM, Hitachi S-4800). The aluminum oxide hydroxide/AT was dispersed in water in ultrasonic bath for 5 min before the FESEM examination.

The Brunauer–Emmett–Teller (BET) surface area and other textural properties were measured by N_2 adsorption-desorption isotherms at 77 K on a micromeritics ASAP 2020 instrument. Surface areas were calculated using the BET equation, and pore size distributions were calculated using the Barrett–Joiner–Halenda (BJH) model based on nitrogen desorption isotherms.

Wide angle X-ray diffraction (XRD) was respectively performed on powders of aluminum oxide hydroxide/AT, AT, and aluminum hydroxide by a Rigaku D/max-2550 PC X-ray diffractometer with a Cu K_α ($\lambda = 0.154056$ nm) radiation source at a generator voltage of 40 kV and a generator current of 200 mA.

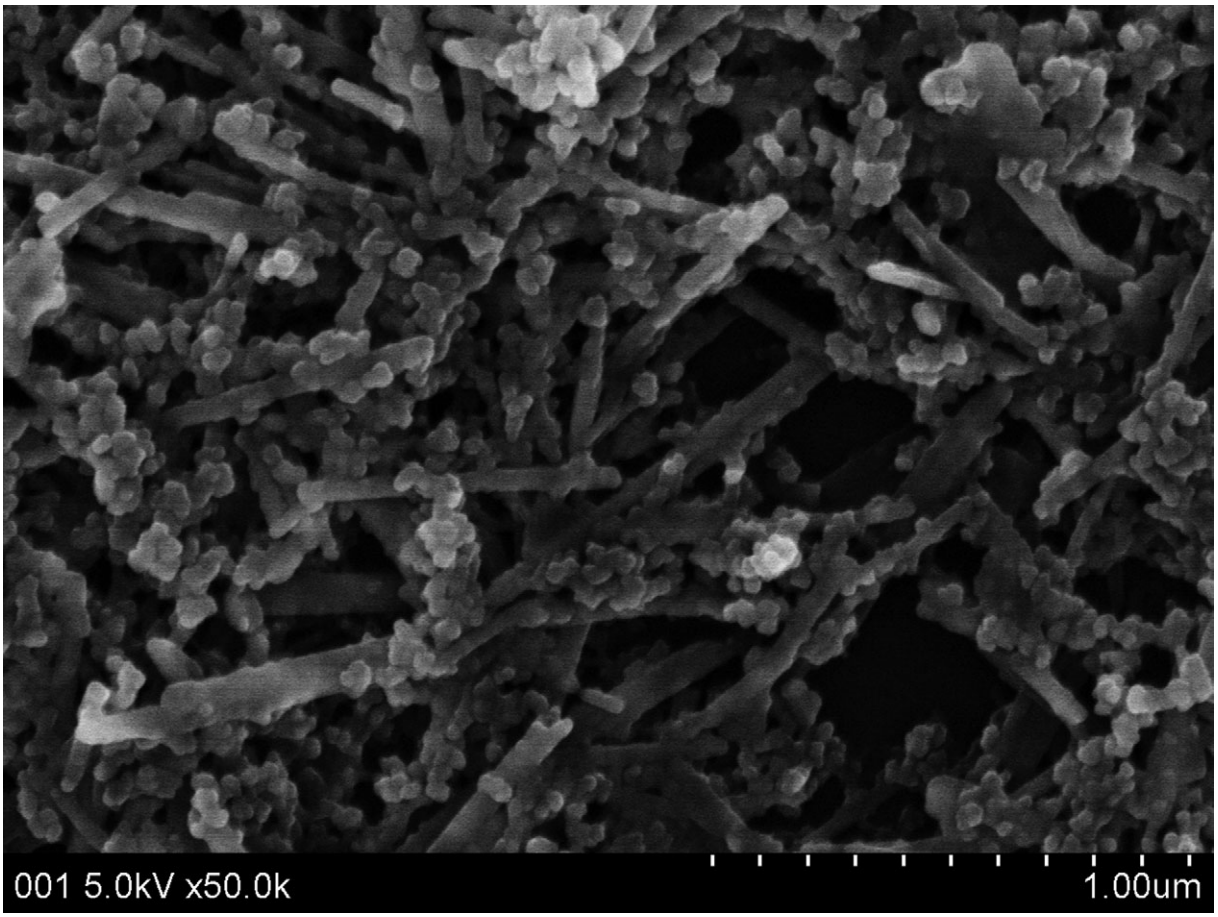

Figure 1. FESEM image of Aluminum oxide hydroxide/AT.

Catalyst Activity Test

In this method, BHET is mixed with the catalyst under investigation and a small sample (1–15 mg) is placed in the sample cell of the measuring head of DSC. Due to technical limitations, it was difficult to weigh an amount of catalyst corresponding to 6667 ppm in 15 mg of BHET (<0.1 mg of catalyst). So a larger amount of catalyst–BHET mixture was prepared by uniformly mixing of the desired amount of catalyst and 1.5 g of BHET according to the equal increment way.

After this homogenization process, DSC experiments were carried out using a Q20 thermal analyzer. The polycondensation was carried out by placing a 5 mg sample in a aluminum crucible and heated to 300–350°C at 2.5 K/min, 5 K/min, 10 K/min, and 20 K/min under 50 ml/min nitrogen purging. All these runs were done in aluminum crucibles covered with centrally holed lids.

In the study, the TGA apparatus was coupled to FTIR (Fourier transform infrared spectroscopy) spectrometer in order to identify the evolved gases. TGA was carried out using NETZSCH TG 209 F1 thermogravimetric analyzer by heating to 400°C at 20 K/min under 20 ml/min nitrogen purging. The polycondensation was carried out by placing a small sample (4–10 mg) in a uncovered alumina crucible. A FTIR spectrum was recorded every 10 s in the region of 200–350°C on a Nicolet Nexus-670 spectrometer (Nicolet Instrument Co., USA) over the range of 400–4000 cm^{-1}.

To further verify the above activity tests, the following polymerization test has been done using 1 L polymerizer. The preparation procedure of PET can be divided into two steps. In the first step, the esterification, the reaction of 300 g purified TPA and 160 g EG was carried out in the presence of 0.08 weight% (via TPA) of aluminum hydroxide catalyst, at temperatures in the range from 230°C to 240°C under nitrogen atmosphere. In the second step, the polycondensation reaction was carried out at about 280°C under a pressure of less than 200 Pa. After a reaction time of about 1–2.5 h (the high vacuum stage time), a polymer have a high intrinsic viscosity was obtained. PET was synthesized under the same reaction conditions as mentioned already except that the catalyst was changed.

All the intrinsic viscosity (IV) measurements of the resulting polymer were conducted at 25°C in a Ubbelohde viscometer using phenol/tetrachloroethane (1 : 1, wt/wt) as the solvent. The viscosity-average relative molecular mass $\overline{M}_\eta$ is related to the IV by the following equation:[18]

$$[\eta] = 2.1 \times 10^{-4} \overline{M}_\eta^{\,0.82}. \quad (1)$$

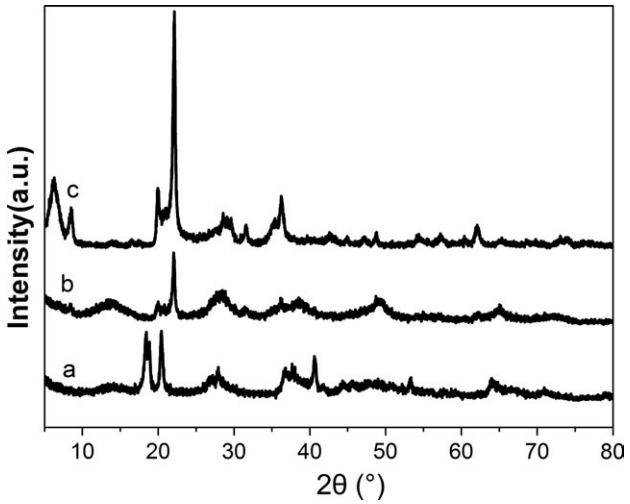

Figure 2. XRD patterns of (a) $Al(OH)_3$, (b) AlO(OH)/AT, and (c) pure AT samples.

RESULTS AND DISCUSSION

Characterization of Catalysts

Figure 1 shows that the diameter of AT is about 100 nm, and the length of AT is between 500–3000 nm. This high length-diameter ratio is favorable to enhance the polymer materials.[11] As shown in Figure 1, numerous approximately spherical nanoparticles can be observed clearly. It indicates that the interactions between the AT single crystal were weakened and the great majority of AT single crystal can be separated by ultrasonication.

Figure 2 shows the XRD patterns of pure AT, aluminum hydroxide, and aluminum oxide hydroxide/AT samples. For the aluminum hydroxide, sharp peaks assignable to gibbsite (JCPDS PDF # 33-0018) were identified, confirming the presence of $Al(OH)_3$. For aluminum oxide hydroxide/AT, there are not only diagnostic diffractions of AT (2θ=21.9°), but also diagnostic diffractions of AlO(OH) at 2θ of 14.0°, 28.2°, 38.4°, 48.8°, 55.2°, 65.0°, and 71.7° (JCPDS PDF#49-0133) were identified, confirming the presence of AlO(OH) in the aluminum oxide hydroxide/AT. However, no diagnostic diffractions of $Al(OH)_3$ were found in the aluminum oxide hydroxide/AT.

According to the results mentioned above, we can infer the formation process of AlO(OH). It is generally believed that $Al(OH)_4^-$ is the main existence form in sodium aluminate solution,[19,20] so the following reactions will be carried out during the preparation of aluminum oxide hydroxide/AT.

$$Na[Al(OH)_4] + HCl\ (small) = Al(OH)_3 \downarrow + NaCl + H_2O, \quad (2)$$

Table I. BET Surface Area and Pore Size

Test samples	BET surface area (m^2/g)	Pore volume (cm^3/g)	Pore diameter (nm)
$Al(OH)_3$	329.3	0.220	3.4
AT	86.6	0.359	15.8
AlO(OH)/AT	153.6	0.118	3.3

$$Al(OH)_3 \rightleftharpoons AlO(OH) + H_2O. \quad (3)$$

During the drying process of aluminum oxide hydroxide/AT, the balance in eq. (3) will shift to the right under the action of AT, which is favorable to form the crystal structure of AlO(OH). The amount of AlO(OH) can be calculated according to the number of moles of aluminum atoms in the sodium aluminate solution. Assuming that the quality loss of catalyst can be neglected during the process of preparation, the theoretical mass fraction of catalyst load on AT can be estimated as follows.

$$\frac{m_{AlO(OH)}}{m_{AlO(OH)} + m_{AT}} = \frac{(4.1/82) \times 60}{(4.1/82) \times 60 + 1} \times 100\% = 75\%. \quad (4)$$

The BET surface areas of the $Al(OH)_3$, AT, and AlO(OH)/AT samples are presented in Table I. It can be seen from Table I that the as-prepared catalysts show high surface areas. The surface area of $Al(OH)_3$ sample was much higher than that of AT under the test condition. This phenomenon was due to a microporous structure from the transformation of $Al(OH)_3$ particles during the thermal treatment.

Catalyst Activity

TGA-IR Analysis. The basic reaction of BHET polycondensation is shown in Scheme 1. The reaction equilibrium can be moved to the right by removing the EG produced in the polycondensation.

Figure 3 depicts the TGA and derivative thermogravimetry (DTG) curves of BHET-AlO(OH)/AT sample. The DTG curve was obtained by plotting the first derivative of mass loss with respect to temperature versus temperature, and it represents mass loss rate. It can be seen from Figure 3 that the first step degradation of BHET has a maximum in the DTG curve at about 579.7 K.

Figure 4 shows FTIR spectra of evolved gas of BHET polycondensation at the temperature which the DTG peak correspond to the maximum reaction rate. It can be seen from Figure 4 that the appearance of both absorption bands at 2967.91 and 2909.91 cm^{-1} is respectively attributed to the characteristic band of the asymmetric and symmetric stretching vibration of the methylene C—H bond; the appearance of both absorption bands at 1393.38 and 1406.84 cm^{-1} is attributed to the characteristic band of the bending vibration of the methylene C—H bond; the appearance of the absorption band at 898.28 cm^{-1} is attributed to the characteristic band of the rocking vibration of the two methylene attached to C—C bond; the appearance of both absorption bands at 1250.02 and 1047.45 cm^{-1} is

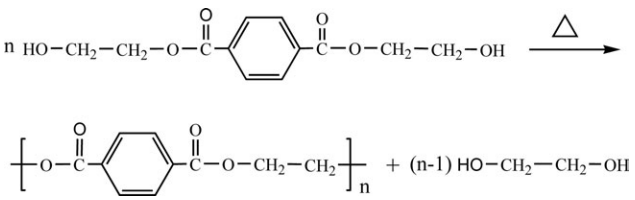

Scheme 1. BHET polycondensation to PET.

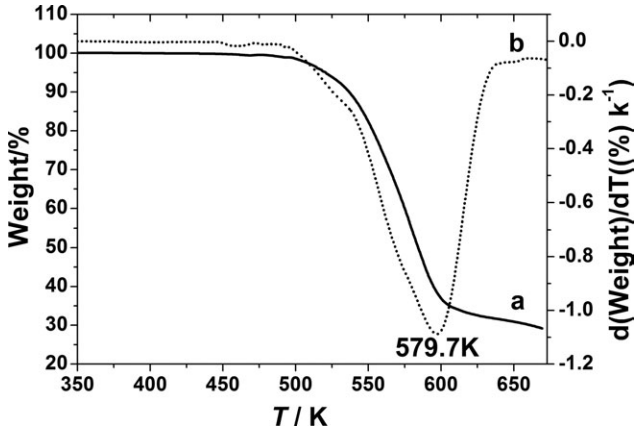

Figure 3. (a) TGA curve and (b) DTG curve of BHET-AlO(OH)/AT sample.

attributed to the characteristic band of the stretching vibration of the C—O bond of alcohol group; the appearance of absorption band at 3674.17 cm^{-1} is attributed to the characteristic band of the stretching vibration of the O—H bond of hydroxyl group; absorption bands at both 4000–3500 and 2000–1500 cm^{-1} are attributed to the water (background moisture). They prove the existence of EG in the escape product. FTIR spectra of evolved gas at other reaction temperature can also prove the existence of EG. All the results show that AT-supported aluminum oxide hydroxide catalyst can be used to catalyze BHET polycondensation under the applied conditions.

DSC Analysis. Figure 5 depicts the DSC plots obtained in the absence of the catalysts. The DSC method is based on the heat changes during the polycondensation. The first peak at about 385 K corresponds to the melting of BHET. This peak is basically unchanged under the different heating rate. The second peak was due to BHET polycondensation reaction. The peak represents the heat of evaporation of EG evolved during polycondensation. At the second peak summit, the reaction reaches its maximum. The position of the maximum peak is different. It not only depends on the catalyst but also depends to some extent on the heating rate. If reactants are consumed earlier, maximum rate will also occur earlier and consequently peak temperature (T_p) will have smaller values.[15] It can be seen from Figure 5 that AlO(OH)/AT catalyst is much more active than $Al(OH)_3$.

Kinetic Analysis. To simplify the treatment of the experimental data and to increase the accuracy of the results, the study will be focused on the effect of different catalysts on the major polycondensation reaction. A new method was built to evaluate the catalyst activity. Generally, the higher the activation energy, the harder it is for a reaction to occur and vice versa. The catalyst activity for BHET polycondensation was mainly influenced by the apparent activation energy. AT support can influence the apparent activation energy of BHET polycondensation, which will be proved by the following activation energy calculating results.

Many mathematical models based on the TGA and DSC data have been developed to determine the activation energy. In this article, the activation energy was calculated based on the DSC data by using the Starink[21,22] method regardless of the rate expressions of reactions and was further determined by a procedure of iterative calculations.

The basic reaction (see Scheme 1) can be considered irreversible when EG was removed. In isothermal analyses, the reaction rate equation is expressed as follows.

$$\frac{d\alpha}{dt} = kf(\alpha), \tag{5}$$

where α, the degree of conversion, equals the amount transformed at time t divided by the maximum amount that can transform before equilibrium is reached ($t\rightarrow\infty$); $f(\alpha)$, the reaction mechanism function; and k, the reaction rate constant. The reaction rate constant might be expressed by the Arrhenius equation.

$$k = A\exp(-E/RT), \tag{6}$$

where A is the pre-exponential factor of the Arrhenius equation; E, apparent activation energy; R, the molar gas constant; and T, the absolute temperature at time t.

Assuming that the non-isothermal reaction is similar to an isothermal reaction in an infinitesimal time, the reaction rate equation of the non-isothermal reaction may be expressed as follows.

$$\frac{d\alpha}{dT} = \frac{A}{\beta}f(\alpha)\exp(-E/RT), \tag{7}$$

where β is the constant heating rate.

The following assumptions are permitted, namely that, assume that A, $f(\alpha)$, and E are independent of T and that A and E are independent of α, and then one may separate the variables and integrate to obtain eq. (8).[23]

$$G(\alpha) = \int_0^{\alpha}\frac{d\alpha}{f(\alpha)} = \frac{A}{\beta}\int_{T_0}^{T}\exp(-E/RT)dT, \tag{8}$$

where $G(\alpha)$ represents the integration form of the reaction mechanism function, T_0 is the value of T at $t=t_0$. Ordinarily,

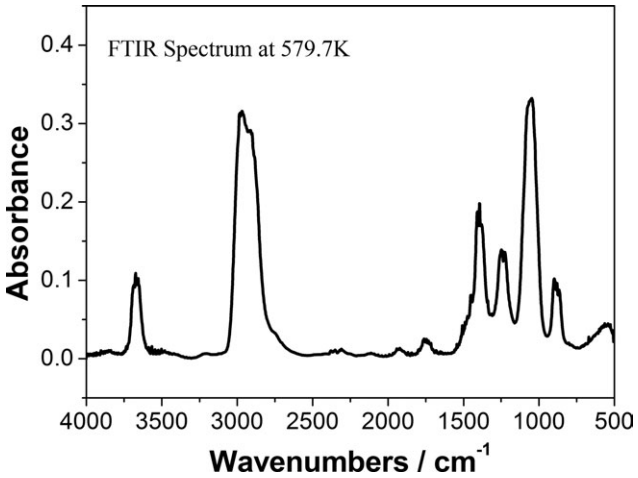

Figure 4. FTIR spectra of evolved gas of the BHET polycondensation.

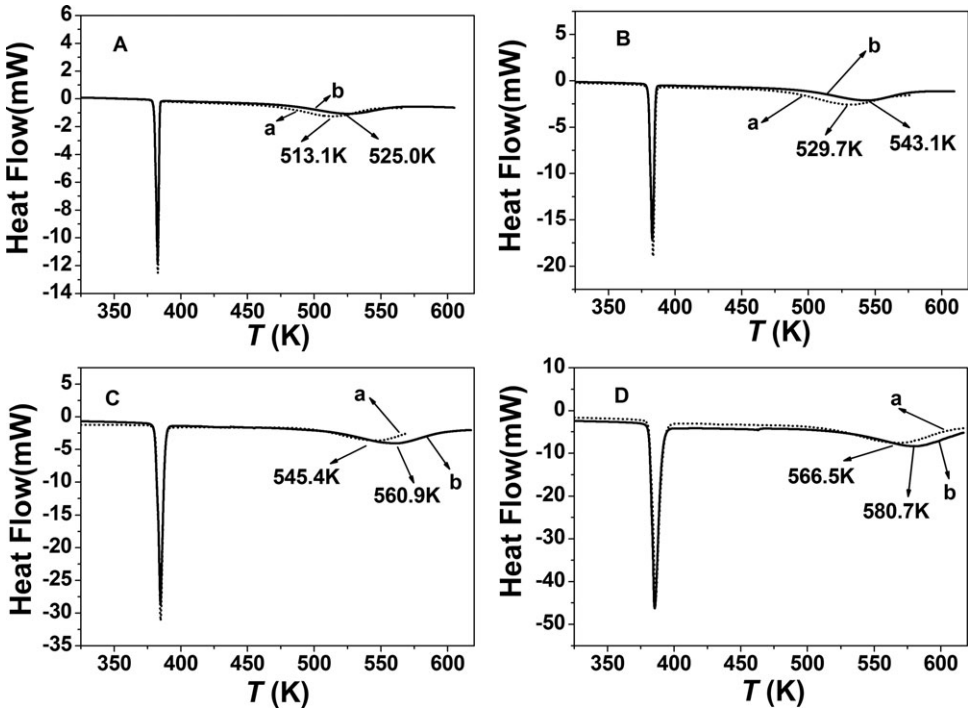

Figure 5. DSC curves of the BHET-catalyst mixture (a, AlO(OH)/AT catalyst; b, $Al(OH)_3$ catalyst); heating rate: (A) 2.5 K/min, (B) 5 K/min, (C) 10 K/min, and (D) 20 K/min.

the rate of the polycondensation reaction is negligible at low temperatures, so the following approximation is valid.

$$\int_{T_0}^{T} \exp(-E/RT)\, dT = \int_{0}^{T} \exp(-E/RT)\, dT. \tag{9}$$

As is well known, the above integral expression has no analytical solution. To obtain approximate analytical solutions, $G(\alpha)$ can be derived as follows.

$$G(\alpha) = \int_0^{\alpha} \frac{d\alpha}{f(\alpha)} = \frac{A}{\beta}\int_0^{T} \exp(-E/RT)dT = \frac{AE}{\beta R}\int_{\infty}^{x} \frac{-e^{-x}}{x^2}dx = \frac{AE}{\beta R}p(x), \tag{10}$$

where $p(x) = \int_{\infty}^{x} \frac{-e^{-x}}{x^2}dx$; $x = \frac{E}{RT}$.

For $15 \leq x \leq 60$, the following approximation form has been obtained.[21]

$$p(x) \cong \frac{\exp(-Bx - D)}{x^S}, \tag{11}$$

where S is a constant, B is a constant which depends on the choice of S, and D is a constant depending on S.

For x lying between 5 and 200, the more exact approximation of $p(x)$ was regarded as eq. (12).[24]

$$p(x) \cong \frac{\exp(-x)}{x^2} Q(x), \tag{12}$$

Table II. Absolute Temperature Versus the Degree of Conversion

	Reaction based on $Al(OH)_3$ catalyst				Reaction based on AlO(OH)/AT catalyst			
α	$T_{\beta=2.5}$ (K)	$T_{\beta=5}$ (K)	$T_{\beta=10}$ (K)	$T_{\beta=20}$ (K)	$T_{\beta=2.5}$ (K)	$T_{\beta=5}$ (K)	$T_{\beta=10}$ (K)	$T_{\beta=20}$ (K)
0.1	485.4	500.2	516.8	538.1	475.4	494.9	511.5	527.9
0.2	498.6	514.8	531.0	551.2	488.3	506.6	521.6	540.1
0.3	507.0	523.9	540.3	559.9	496.5	514.3	528.7	548.5
0.4	513.8	530.9	547.7	566.9	502.8	520.5	534.7	555.5
0.5	519.7	537.1	554.2	573.0	508.3	526.0	540.0	561.8
0.6	525.3	542.9	560.4	578.7	513.4	531.4	545.1	567.9
0.7	531.0	548.8	566.6	584.3	518.6	536.8	550.1	574.0
0.8	537.4	555.4	573.7	590.4	524.3	542.9	555.3	580.8
0.9	545.8	564.4	583.2	598.0	531.9	550.9	561.5	589.3

Table III. Activation Energy Calculated by the Use of the Plot of ln ($\beta/hT^{1.92}$) Versus $1/T$

	$Al(OH)_3$		AlO(OH)/AT	
α	E_0 (kJ/mol)	E_1 (kJ/mol)	E_0 (kJ/mol)	E_1 (kJ/mol)
0.1	77.6	77.7	74.6	74.7
0.2	82.4	82.5	80.9	81.0
0.3	84.8	84.9	83.4	83.5
0.4	86.5	86.6	84.6	84.7
0.5	88.1	88.2	85.2	85.2
0.6	89.8	89.9	85.5	85.6
0.7	91.7	91.8	85.9	86.0
0.8	93.9	94.0	86.3	86.4
0.9	97.4	97.5	87.3	87.4
Mean	88.0	88.1	83.7	83.8

where

$$Q(x) = \frac{x^3 + 10x^2 + 18x}{x^3 + 12x^2 + 36x + 24}. \quad (13)$$

The ratio of the exact approximation of $p(x)$ to eq. (11) is defined as $H(x)$.

$$H(x) = \frac{\exp(-x)Q(x)/x^2}{\exp(-Bx - D)/x^S}. \quad (14)$$

Thus,

$$G(\alpha) = \frac{AE}{\beta R}p(x) \cong \frac{AE}{\beta R}H(x)\exp(-Bx - D)/x^S. \quad (15)$$

After taking $H(x)$ into account, exact values for the activation energy can be obtained by an iterative calculation. The iterative equation is as follows.

$$\ln\frac{\beta}{hT^S} \cong \ln\left(\frac{AR^{S-1}}{E^{S-1}G(\alpha)}\right) - \frac{BE}{RT}, \quad (16)$$

where

$$h = H(x)\exp(-D). \quad (17)$$

For $20 < x < 60$, the following highly accurate approximation has been obtained.[22]

$$p(x) \cong \frac{\exp(-1.0008x - 0.312)}{x^{1.92}}. \quad (18)$$

Using eq. (18), the following equation can be derived.

$$\ln\frac{\beta}{T^{1.92}} = \ln\left(\frac{AR^{0.92}}{E^{0.92}G(\alpha)}\right) - \frac{1.0008E}{RT} - 0.312. \quad (19)$$

By using eq. (19), for the same α, the initial value of the activation energy E_0 can be calculated from the plot of ln ($\beta/T^{1.92}$) versus $1/T$.

Using eq. (16), the following equation can be obtained.

$$\ln\frac{\beta}{hT^{1.92}} \cong \ln\left(\frac{AR^{0.92}}{E^{0.92}G(\alpha)}\right) - \frac{1.0008E}{RT}, \quad (20)$$

where

$$h = H(x)\exp(-0.312). \quad (21)$$

The iterative procedure can be summarized as follows.[25]

Step 1: using E_0 calculate x and h, then from eq. (20) calculate a new value E_1 for the activation energy from the plot of ln ($\beta/hT^{1.92}$) versus $1/T$.

Step 2: repeat step 1, replacing E_0 with E_1. And so on until the absolute difference of ($E_i - E_{i-1}$) is less than a defined small quantity such as 0.1 kJ/mol generally. The last value E_i is the exact value of activation energy of the reaction.

As the mechanism function of the reaction was unknown, we kept the initial mass of sample at a fixed constant in all DSC measurements in order to ignore the effect of the initial mass of sample on calculation of kinetic parameters. The following calculation of activation energy was carried out based on DSC data.

For DSC analysis, the following relation is true.[26]

$$\alpha = \frac{H}{H_0}, \quad (22)$$

where H_0 is the total reaction enthalpy and H is the reaction enthalpy from the beginning to time t. The absolute temperature, T, versus the degree of conversion, α, was shown in Table II.

For the fixed α, the initial value of the activation energy E_0 can be estimated by use of the plot of ln ($\beta/T^{1.92}$) versus $1/T$ from Table II, and the last value of the activation energy can be further determined by use of the plot of ln ($\beta/hT^{1.92}$) versus $1/T$.

All the calculated results of the activation energy were indicated in Table III. It can be seen from Table III that the average value

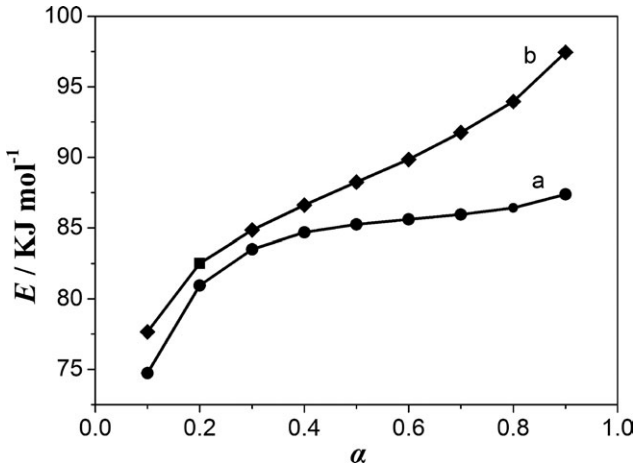

Figure 6. The relationship of the activation energy versus degree of conversion: (a) AlO(OH)/AT catalyst and (b) $Al(OH)_3$ catalyst.

Table IV. Polycondensation Time and Intrinsic Viscosity of PET Chip

Catalyst	Amount of catalyst (weight %, via TPA)	Polycondensation time (min)	Intrinsic viscosity (dL/g)	Viscosity-average molecular weight (g/mol)
$Al(OH)_3$	0.08	100	0.572	1.55×10^4
AlO(OH)/AT	0.08	90	0.631	1.74×10^4
$Al(OH)_3$	0.09	95	0.603	1.65×10^4
AlO(OH)/AT	0.09	85	0.661	1.84×10^4

of apparent activation energy of AlO(OH)/AT catalyst was lower about 4.3 kJ/mol than that of $Al(OH)_3$.

Figure 6 shows that the activation energy of $Al(OH)_3$ catalyst has a significant change with the degree of conversion, and AlO(OH)/AT catalyst is more active than $Al(OH)_3$.

The Verification of Catalyst Activity. In general, under the same polycondensation temperature and time, the higher the intrinsic viscosity, the more activity is for a polycondensation catalyst. It can be seen from Table IV that the catalytic activity of AlO(OH)/AT is higher than that of $Al(OH)_3$. According to Refs. 27 and 28, a reaction mechanism might be proposed to explain the aluminum-based catalyst. After considering the effect of hydroxyl group on the AT surface, the reaction mechanism might be described in Scheme 2. It can be seen from Scheme 2 that the hydroxyl group on the AT surface has a synergistic effect on aluminum ion, which can increase the catalyst activity.

CONCLUSIONS

This work demonstrates that AT-supported aluminum oxide hydroxide catalyst is effective in catalyzing BHET polycondensation.

The intrinsic viscosity of PET product obtained by using AlO(OH)/AT catalyst can reach more than 0.65 dL/g within a shorter time, while the catalyst amount was smaller than $Al(OH)_3$ amount.

A more accurate method for calculating the activation energy was presented. The activation energy can be applied to evaluate the catalyst activity. Under identical reaction conditions, the average value of apparent activation energy of AlO(OH)/AT catalyst was lower about 4.3 kJ/mol than that of $Al(OH)_3$.

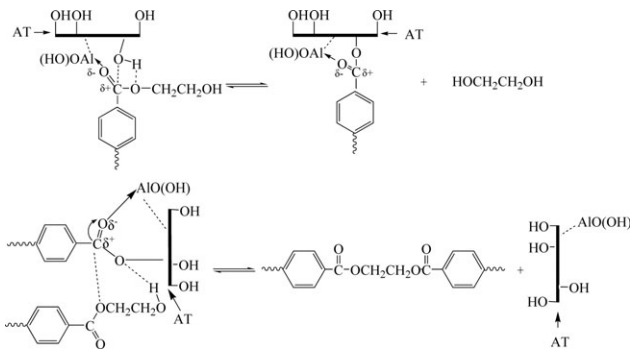

Scheme 2. The reaction mechanism based on AlO(OH)/AT catalyst.

Considering the environmentally friendly preparation method and the lower cost, the AlO(OH)/AT catalyst can be a promising candidate to replace Sb catalyst in the near future.

ACKNOWLEDGMENTS

This work was supported by the Program of Introducing Talents of Discipline to Universities (No. 111-2-04).

REFERENCES

1. Biros, S. M.; Bridgewater, B. M.; Villeges-Estrada, A.; Tanski, J. M.; Parkin, G. *Inorg. Chem.* **2002**, *41*, 4051.
2. Dou, J. Y.; Liu, Z. P. *Green Chem.* **2012**, *14*, 2305.
3. Finelli, L.; Lorenzetti, C.; Messori, M.; Sisti, L.; Vannini, M. *J. Appl. Polym. Sci.* **2004**, *92*, 1887.
4. Macdonald, W. *Polym. Int.* **2002**, *51*, 923.
5. Yin, M.; Li, C. C.; Guan, G. H.; Zhang, D.; Xiao, Y. N. *J. Appl. Polym. Sci.* **2010**, *115*, 2470.
6. Thiele, U. U.S. Patent 5,733,969, March 31, **1998**.
7. Goodley, G. R. U.S. Patent 5,596,069, January 21, **1997**.
8. Nakajima, T.; Tsukamoto, K.; Gyobu, S.; Kuwata, M. Eur. Pat. 1,227,117, July 31, **2002**.
9. Haden, W. L.; Schwint, L. A. *Ind. Eng. Chem.* **1967**, *59*, 58.
10. Yao, X. Y.; Tian, X. Y.; Zhang, X.; Zheng, K.; Zheng, J.; Zhang, H. B.; Chen, L.; Li, Y.; Cui, P. *J. Appl. Polym. Sci.* **2008**, *110*, 140.
11. Yuan, X. P.; Li, C. C.; Guan, G. H.; Liu, X. Q.; Xiao, Y. N.; Zhang, D. *J. Appl. Polym. Sci.* **2007**, *103*, 1279.
12. Zuo, Z. J.; Huang, W.; Han, P. D.; Gao, Z. H.; Li, Z. *Appl. Catal. A* **2011**, *408*, 130.
13. Wolf, K. H.; Kuester, B.; Herlinger, H.; Tschang, C. J.; Schollmeyer, E. *Angew. Makromol. Chem.* **1978**, *68*, 23.
14. Gamlen, G. A.; Shah, T. H.; Bhatty, J. I.; Dollimore, D. *Thermochim. Acta* **1986**, *106*, 105.
15. El-Toufaili, F. A.; Wiegner, J. P.; Feix, G.; Reichert, K. H. *Thermochim. Acta* **2005**, *432*, 99.
16. Coelho, A.; Fonseca, I. M.; Matos, I.; Marques, M. M.; Botelho do Rego, A. M.; Lemos, M. A. N. D. A.; Lemos, F. *Appl. Catal. A* **2010**, *374*, 170.
17. Gangwal, V. R.; van der Schaaf, J.; Kuster, B. F. M.; Schouten, J. C. *Appl. Catal. A* **2004**, *274*, 275.
18. Kang, C. K. *J. Appl. Polym. Sci.* **1998**, *68*, 837.

19. Lippincott, E. R.; Psellos, J. A.; Tobin, M. C. *J. Chem. Phys.* **1952**, *20*, 536.
20. Radnai, T.; May, P. M.; Hefter, G. T; Sipos, P. *J. Phys. Chem. A* **1998**, *102*, 7841.
21. Starink, M. J. *Thermochim. Acta* **1996**, *288*, 97.
22. Starink, M. J. *Thermochim. Acta* **2003**, *404*, 163.
23. Flynn, J. H.; Wall, L. A. *J. Polym. Sci. Part B: Polym. Lett.* **1966**, *4*, 323.
24. Urbanovici, E.; Popescu, C.; Segal, E. *J. Therm. Anal. Calorim.* **1999**, *55*, 325.
25. Gao, Z.; Nakada, M.; Amasaki, I. *Thermochim. Acta* **2001**, *369*, 137.
26. Zhang, T. L.; Hu, R. Z.; Li, F. P. *Thermochim. Acta* **1994**, *244*, 177.
27. Duh, B. *Polymer* **2002**, *43*, 3147.
28. Apicella, B.; Di-Serio, M.; Fiocca, L.; Po, R.; Santacesaria, E. *J. Appl. Polym. Sci.* **1998**, *69*, 2423.